Advancing Beauty Reconstruction with HGNNs

William Sutcliffe

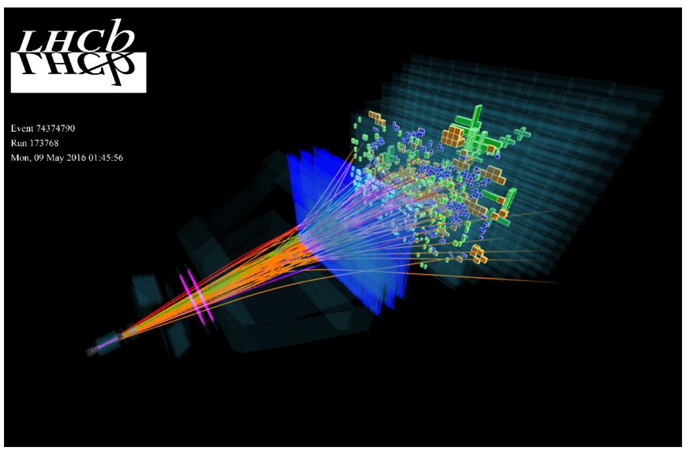

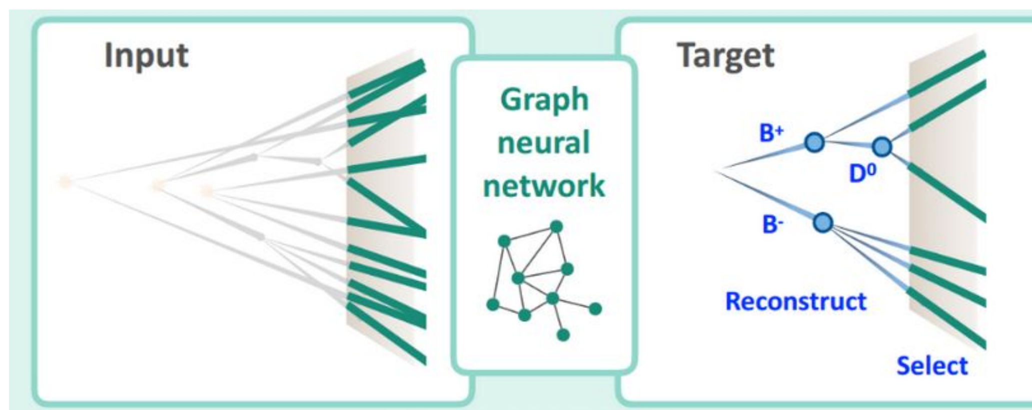

EUCAIF Sardinia

19/06/25

Universität Zürich UZH

Motivation

- Growing luminosity at LHCb is challenging beauty hadron reconstruction
  - higher particle multiplicities mean more background
  - overlapping pp-collisions leading to primary vertex (PV) misassociation.
- Stringent latency and storage requirements for data acquisition.
- Inclusive approach for storing relevant parts of the event necessary.

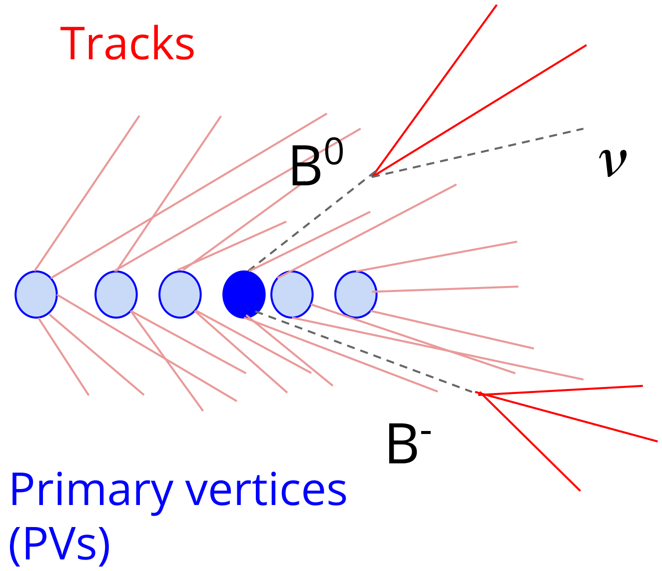

LHCb period	Num. vis. pp collisions	Num. tracks	Num. b hadrons	Num. c hadrons
Runs 1–2	~ 1	~ 50	$\ll 1$	$\ll 1$
Runs 3–4 (Upgrade I)	~ 5	~ 150	$\ll 1$	~ 1
Runs 5 (Upgrade II)	~ 50	~ 1000	~ 1	~ 5

Only objects in LHCb geometrical acceptance are considered

Deep Full Event Interpretation (DFEI)

Julian Garcia Pardinas, Marta Calvi, Rafael Silva Coutinho, Jonas Eschle, Abhijit Mathad, Andrea Mauri, Simone Meloni, Martina Mozzanica, Nicola Serra, Felipe Luan Souza De Almeida, William Sutcliffe, Azusa Uzuki

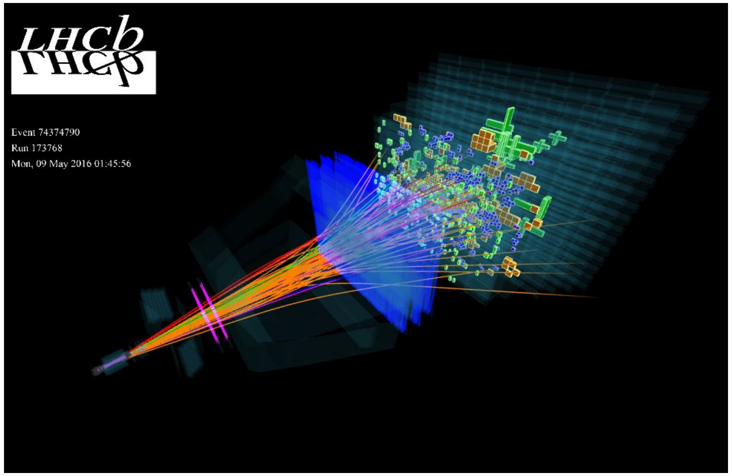

- Previous multi-stage GNN effort [García Pardiñas, J., Calvi, M., Eschle, J. et al. Comput Softw Big Sci 7, 12 (2023).]
- Two main applications of trigger and offline analysis.

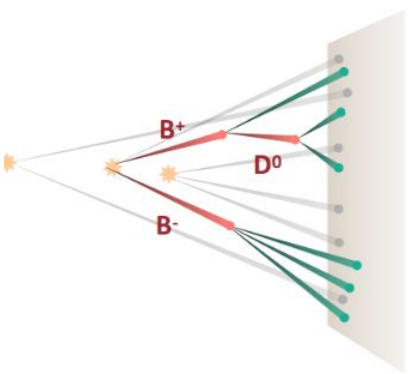

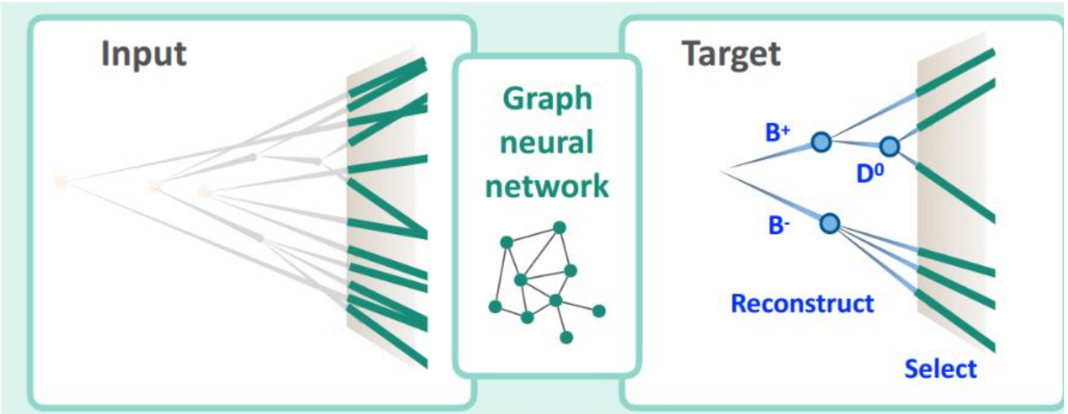

[arXiv:1806.01261v3]

Previous DFEI algorithm

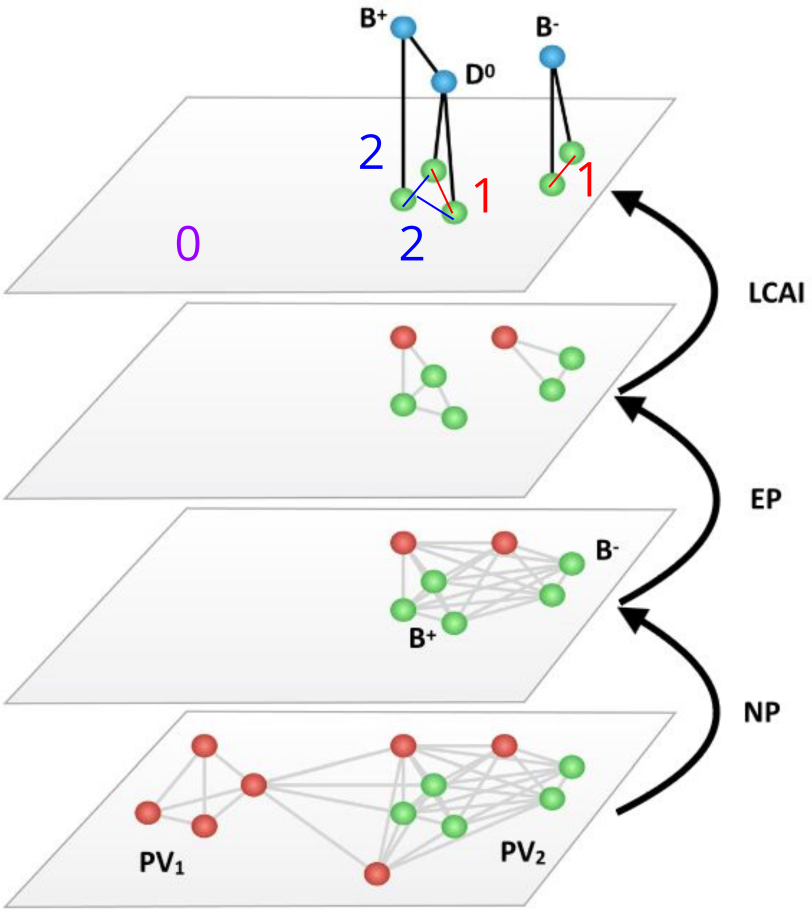

- **Node pruning -** GNN classifies whether node particles are associated with a beauty hadron.

Previous DFEI algorithm

- **Edge pruning -** GNN classifies whether the edges connect particles from the same beauty hadron.

- **Node pruning -** GNN classifies whether node particles are associated with a beauty hadron.

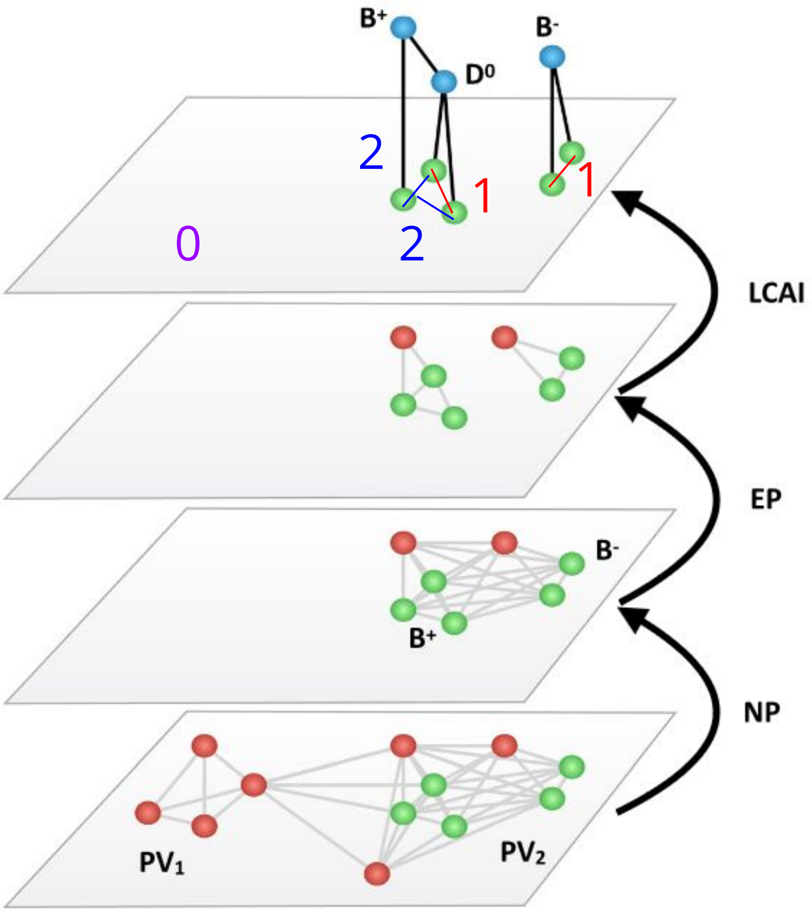

Previous DFEI algorithm

- **Lowest common ancestor (LCA) prediction -** GNN classifies LCA of remaining edges (classes 0,1,2,3).

- **Edge pruning -** GNN classifies whether the edges connect particles from the same beauty hadron.

- **Node pruning -** GNN classifies whether node particles are associated with a beauty hadron.

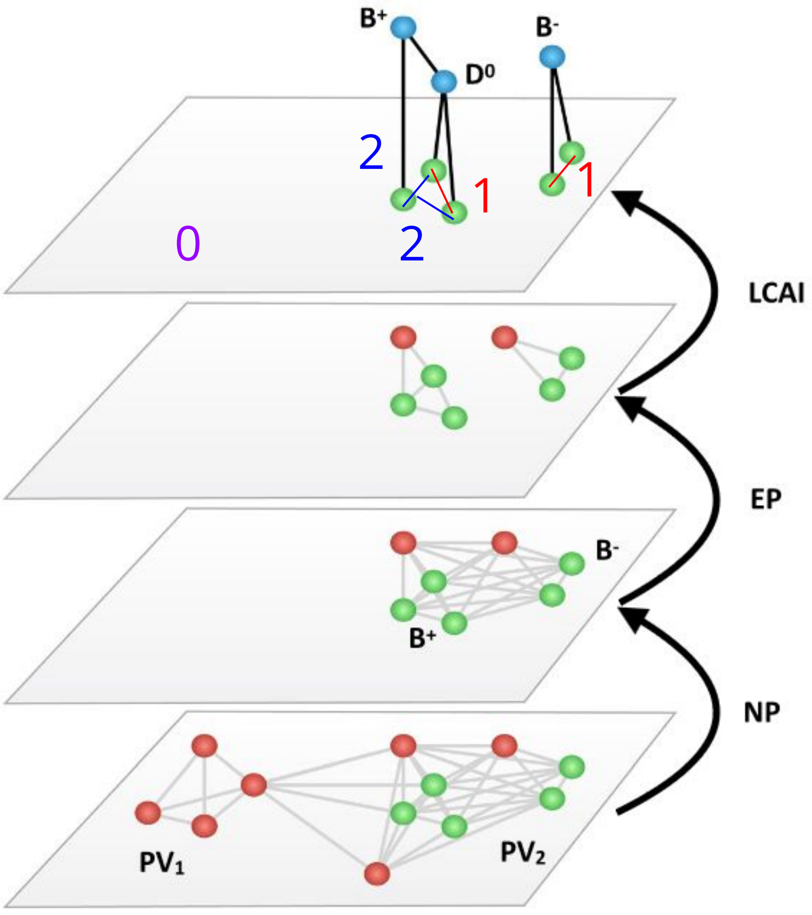

Previous DFEI algorithm

- **Lowest common ancestor (LCA) prediction -** GNN classifies LCA of remaining edges (classes 0,1,2,3).
- **Edge pruning -** GNN classifies whether the edges connect particles from the same beauty hadron.
- **Node pruning -** GNN classifies whether node particles are associated with a beauty hadron.
- Multi-GNN approach high latency.
- PV misassociation not addressed.

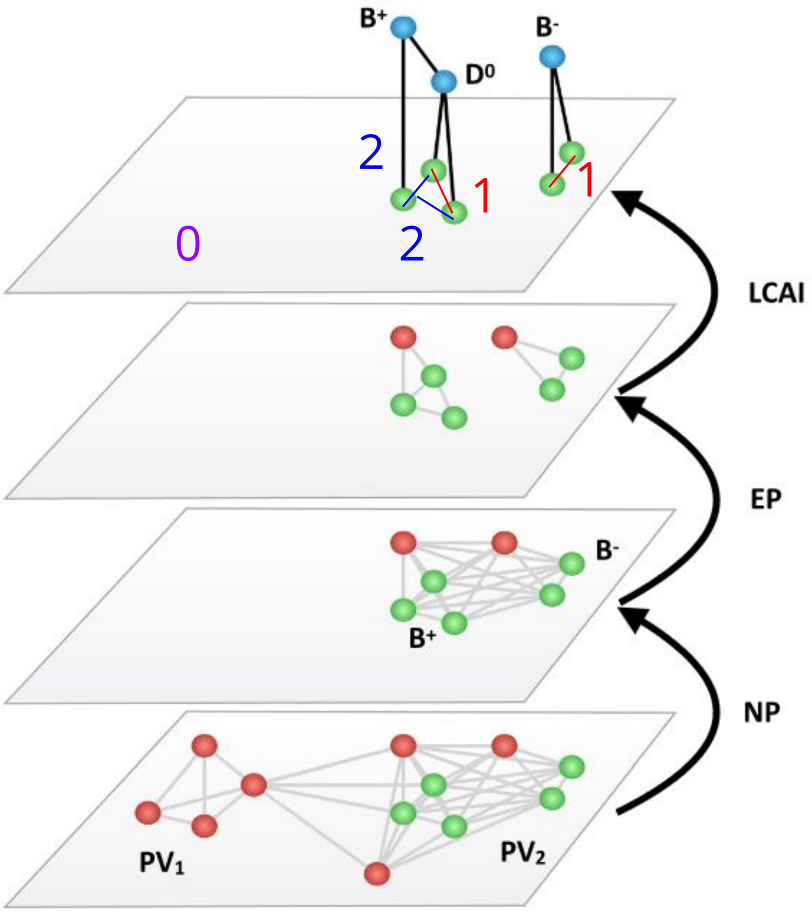

New heterogeneous GNN approach

- Employ a multi-task learning with a HGNN to allow for joint graph pruning, PV association and beauty reconstruction: [arxiv2504.21844]

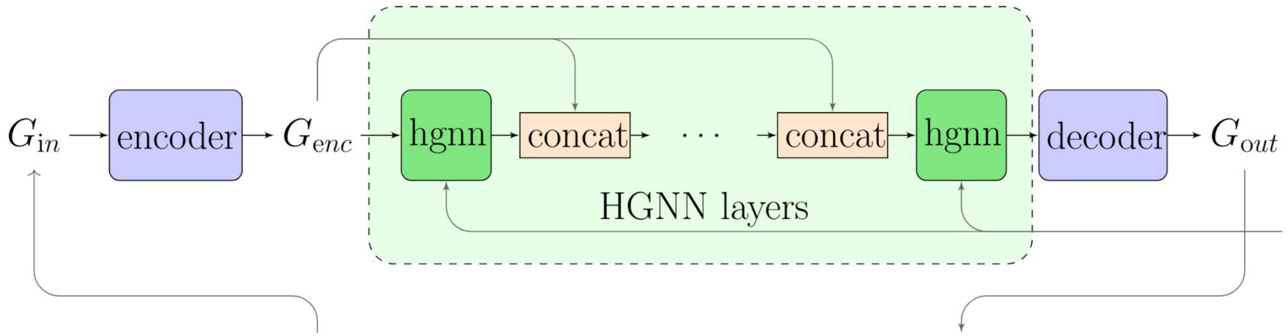

- HGNN layers with integrated pruning for scalability

- Heterogeneous graph representation

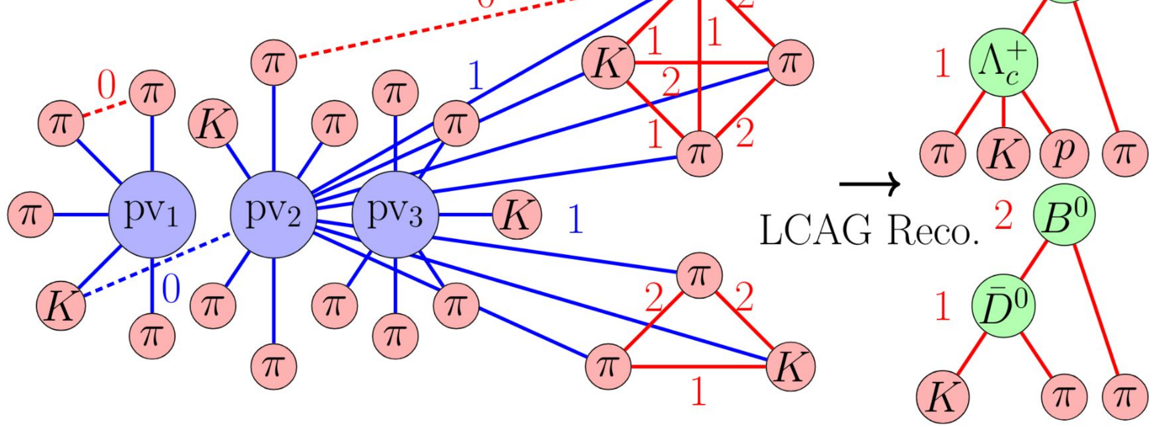

- Train with [custom simulation] ~40k inclusive $pp \; {-}{>} \; b\bar{b}$ events.

- Node and edge features (positions, kinematics, charge)

HGNN layer update

1)

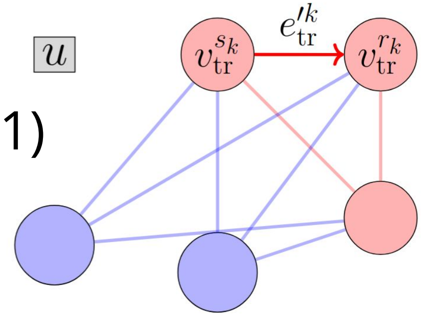

2)

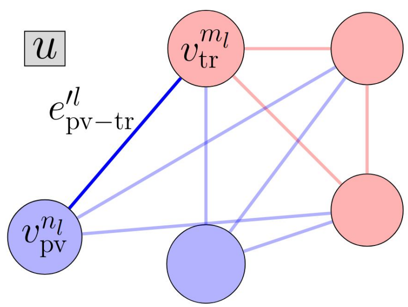

3)

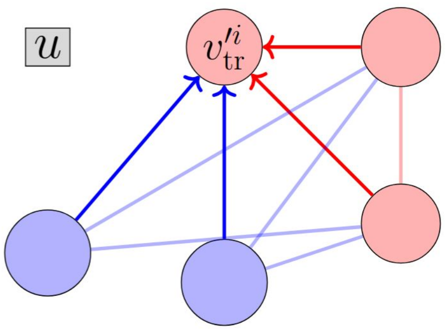

4)

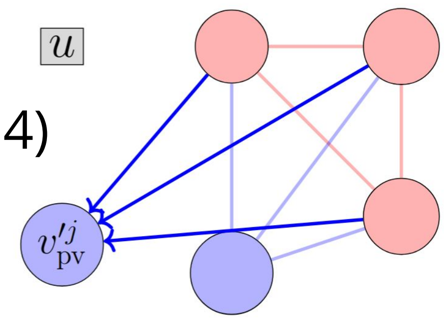

1) $$e'^{k}_{\mathrm{tr}} = \phi^{e_{\mathrm{tr}}}(e^{k}_{\mathrm{tr}}, v^{r_k}_{\mathrm{tr}}, v^{s_k}_{\mathrm{tr}}, u) \qquad \bar{e}'^{i}_{\mathrm{tr}} = \rho^{e_{\mathrm{tr}} \to v_{\mathrm{tr}}}(\{E'^{i}_{\mathrm{tr}}\})$$

2) $$e'^{l}_{\mathrm{pv-tr}} = \phi^{e_{\mathrm{pv-tr}}}(e^{l}_{\mathrm{pv-tr}}, v^{m_l}_{\mathrm{tr}}, v^{n_l}_{\mathrm{pv}}, u) \qquad \bar{e}'^{i}_{\mathrm{pv-tr}} = \rho^{e_{\mathrm{pv-tr}} \to v_{\mathrm{tr}}}(\{E'^{i}_{\mathrm{pv-tr}}\})$$

3) $$v'^{i}_{\mathrm{tr}} = \phi^{v_{\mathrm{tr}}}(v^{i}_{\mathrm{tr}}, \bar{e}'^{i}_{\mathrm{tr}}, \bar{e}'^{i}_{\mathrm{pv-tr}}, u) \qquad \bar{e}'^{j}_{\mathrm{pv-tr}} = \rho^{e_{\mathrm{pv-tr}} \to v_{\mathrm{pv}}}(\{E'^{j}_{\mathrm{pv-tr}}\})$$

4) $$v'^{j}_{\mathrm{pv}} = \phi^{v_{\mathrm{pv}}}(v^{j}_{\mathrm{pv}}, \bar{e}'^{j}_{\mathrm{pv-tr}}, u) \qquad \bar{e}'_{\mathrm{tr}} = \rho^{e_{\mathrm{tr}} \to u}(\{E'_{\mathrm{tr}}\}), \bar{v}'_{\mathrm{tr}} = \rho^{v_{\mathrm{tr}} \to u}(\{V'_{\mathrm{tr}}\})$$

5) $$u' = \phi^{u}(\bar{e}'_{\mathrm{tr}}, \bar{e}'_{\mathrm{pv-tr}}, \bar{v}'_{\mathrm{tr}}, \bar{v}'_{\mathrm{pv}}, u) \qquad \bar{e}'_{\mathrm{tr-pv}} = \rho^{e_{\mathrm{tr-pv}} \to u}(\{E'_{\mathrm{tr-pv}}\}), \bar{v}'_{\mathrm{pv}} = \rho^{v_{\mathrm{pv}} \to u}(\{V'_{\mathrm{pv}}\})$$

5)

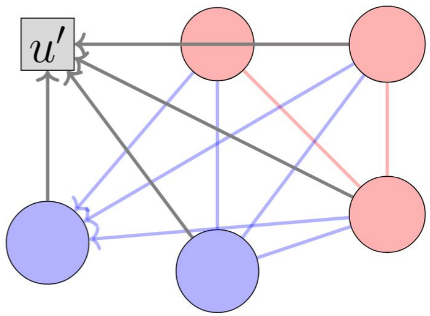

- Based on GNN updates in arxiv1806.01261
- Edge 1), 2) node 2), 3) and global updates (5).
- Edge and node representations, e, v, u
- ϕ = MLP update, ρ = aggregation

Multi-objective loss and pruning

LCA reconstruction, Edge pruning, Node pruning

$$\mathcal{L} = \mathcal{L}_{\mathrm{CE}}\left(e_{\mathrm{out}}, y^{\mathrm{LCA}}\right) + \beta^{e_{\mathrm{tr}}} \sum_{i}^{n_{\mathrm{layers}}^{\mathrm{GNN}}} \mathcal{L}_{\mathrm{BCE}}\left(\hat{y}_i^{e_{\mathrm{tr}}}, y_i^{e_{\mathrm{tr}}}\right) + \beta^{v_{\mathrm{tr}}} \sum_{i}^{n_{\mathrm{layers}}^{\mathrm{GNN}}} \mathcal{L}_{\mathrm{BCE}}\left(\hat{y}_i^{v_{\mathrm{tr}}}, y_i^{v_{\mathrm{tr}}}\right)$$

PV association

$$+ \beta^{e_{\mathrm{pv-tr}}} \sum_{i}^{n_{\mathrm{layers}}^{\mathrm{GNN}}} \mathcal{L}_{\mathrm{BCE}}\left(\hat{y}_i^{e_{\mathrm{pv-tr}}}, y_i^{e_{\mathrm{pv-tr}}}\right)$$

- At each layer compute node and edge scores:

  $\hat{y}^v = \sigma(\psi^v(v')) \quad \hat{y}^e = \sigma(\psi^e(e'))$

  σ=sigmoid, ψ-MLP update

- Constrain scores with BCE loss terms using the ground truth labels

- Removing edges and nodes based on a probability threshold allows for pruning.

- Explore the application of the scores as weights in message passing aggregations, ρ

HGNN Layer computations

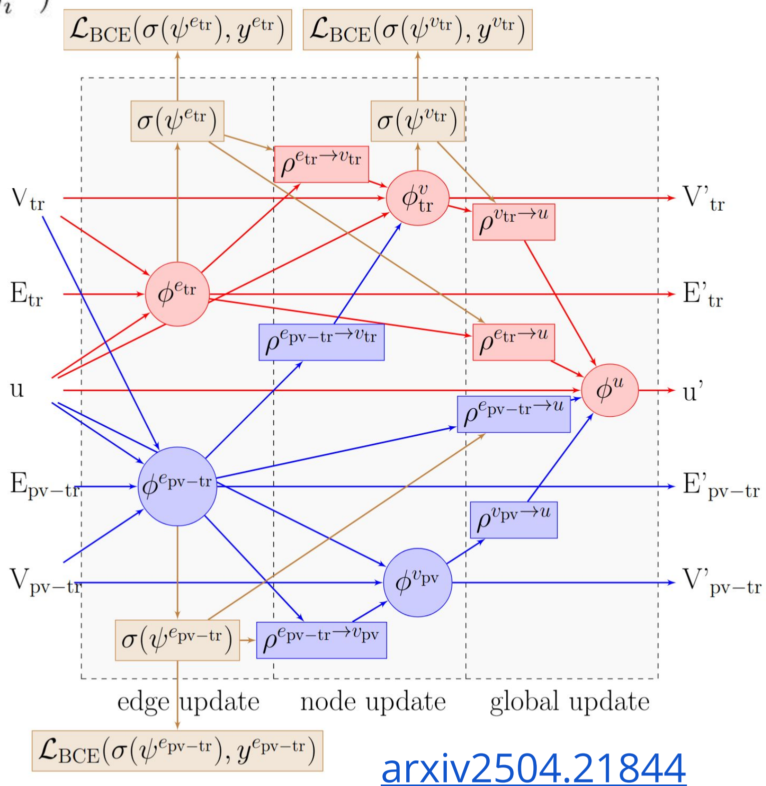

[arxiv2504.21844](https://arxiv.org/abs/2504.21844)

HGNN reconstructed event

- Pruning isolates beauty tracks.
- LCA reconstruction perfectly reconstructs 2 beauty decay chains.
- Association of each track to a PV.

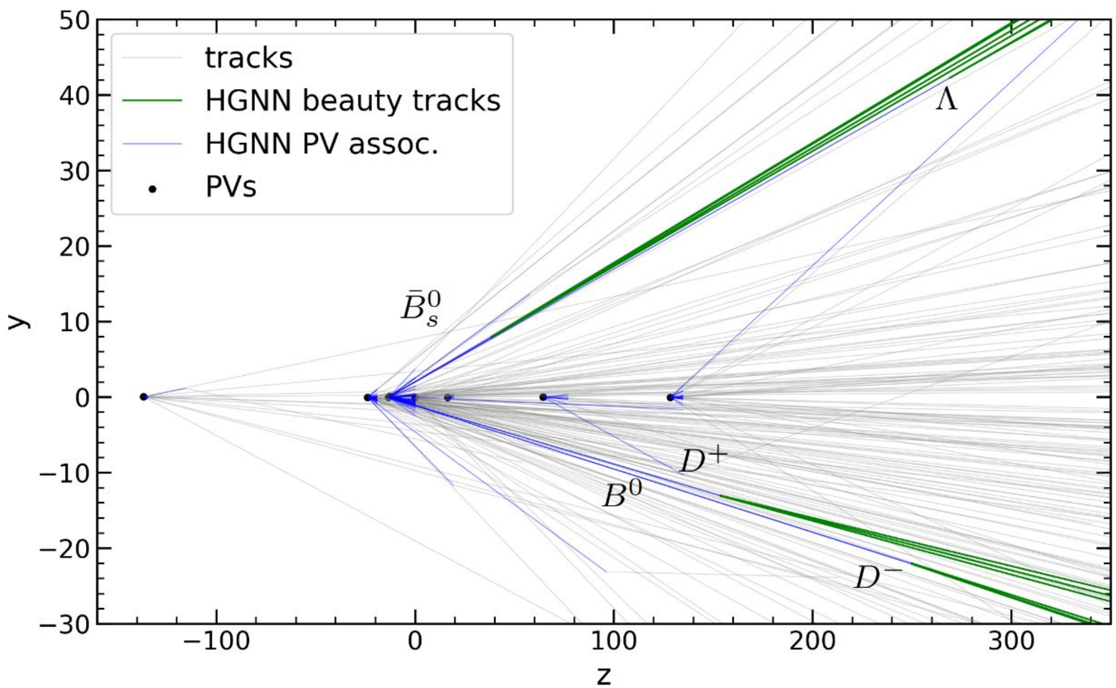

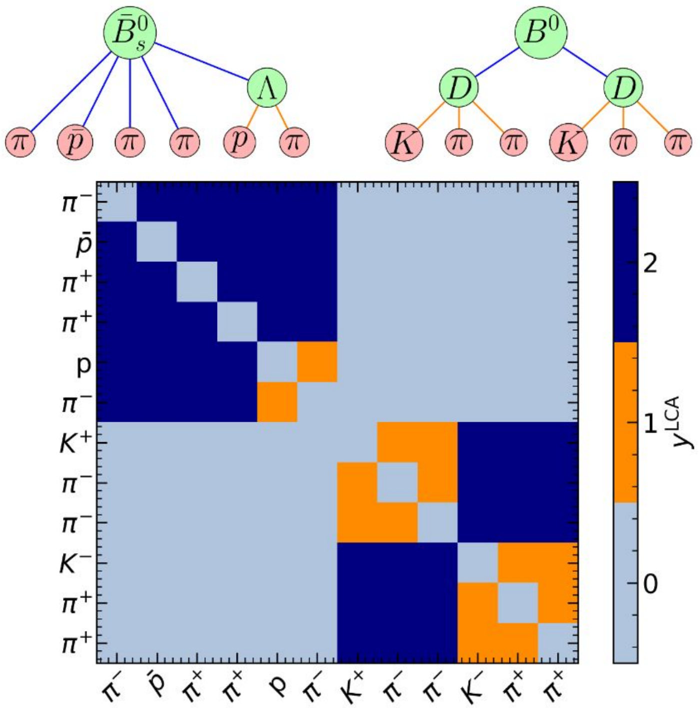

Pruning performance

- Track edge and node pruning performance with layers.

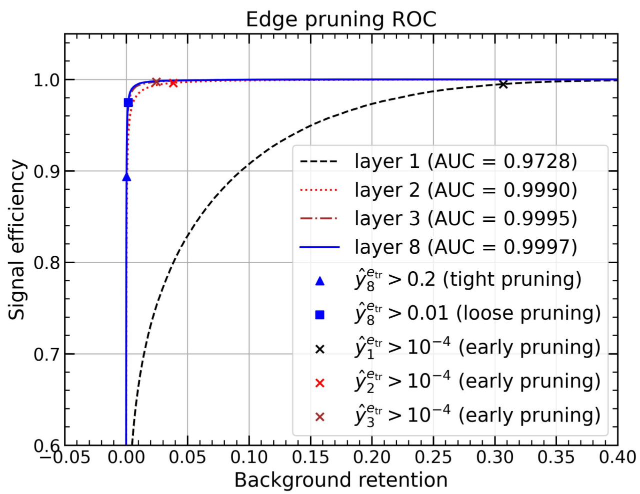

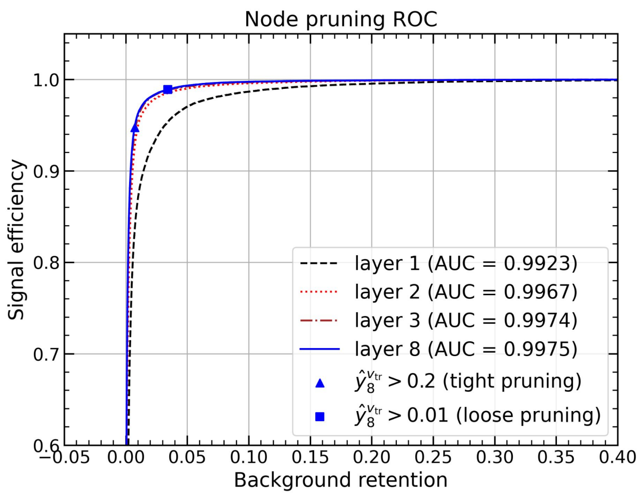

- Tighter pruning reduces background retention at the expense of signal efficiency.
- Signal efficiency stable with growing multiplicity.

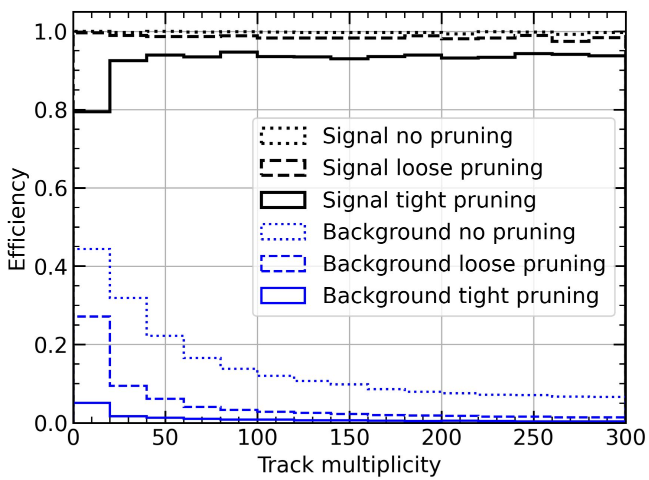

With $y_{LCA}>0$

Reconstruction performance

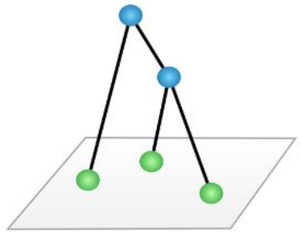

True decay

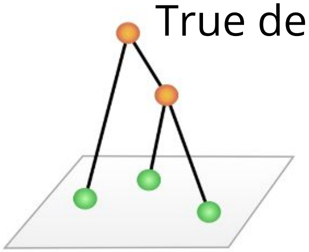

Perfect reco

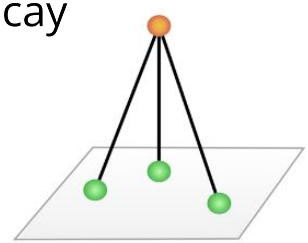

Complete reco

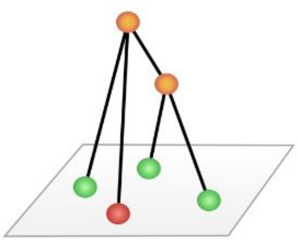

Not isolated

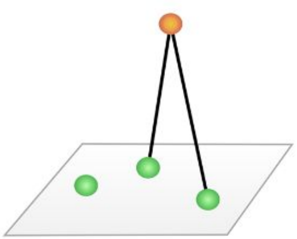

Part. Reco

- Compare DFEI (DF) to nominal HGNN (H1)
- ~5x higher perfect reconstruction

	Perfect reco.			Complete reco.			Not isolated			Part reco.		
Decay	DF	H1	H2	DF	H1	H2	DF	H1	H2	DF	H1	H2
inclusive beauty	4.7	22.4	21.9	6.1	20.1	20.6	76.1	44.1	44.1	13.1	13.4	13.4
$B^0 \to K^{*0}\mu\mu$	32.7	20.3	92.4	17.8	37.7	1.1	43.9	6.2	4.7	5.6	35.8	1.8
$B^0 \to K\pi$	38.1	47.4	91.6	0.0	0.0	0.0	54.7	10.2	7.0	7.2	42.4	1.4
$B^+ \to K\pi\pi$	35.6	23.7	94.5	10.3	26.3	0.2	46.5	8.5	4.7	7.6	41.5	0.6
$B^0_s \to J/\psi\phi$	31.3	22.8	91.8	20.3	44.3	1.7	44.3	9.9	5.0	4.1	22.9	1.5
$\Lambda_b \to \Lambda_c^+\pi$	22.2	27.5	68.3	8.6	9.4	24.4	37.4	7.3	5.2	31.8	55.7	2.1
$B^0 \to K\mu\mu$	36.2	21.0	93.5	10.4	28.1	0.3	45.9	8.4	4.9	7.5	42.5	1.2
$B^0_s \to D_s^-\pi$	33.0	57.7	67.5	7.1	11.6	23.0	53.5	13.1	7.0	6.4	17.6	2.6
$B^0 \to D^+D^-$	26.2	37.1	56.7	23.9	40.2	32.1	45.7	14.3	7.3	4.1	8.4	4.0
$\Lambda_b \to pK$	39.5	24.2	92.3	0.0	0.0	0.0	48.6	5.7	6.4	12.0	70.1	1.3
$\Lambda_b \to pK\mu\mu$	40.9	11.5	94.7	11.1	17.7	0.5	37.4	4.8	3.7	10.6	66.1	1.1

Reconstruction performance

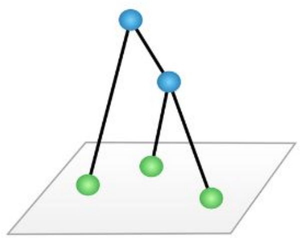

True decay

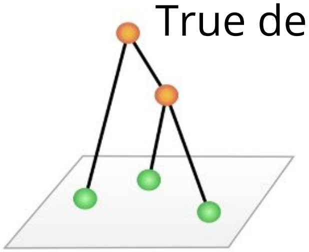

Perfect reco

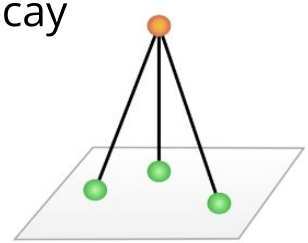

Complete reco

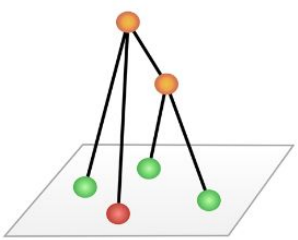

Not isolated

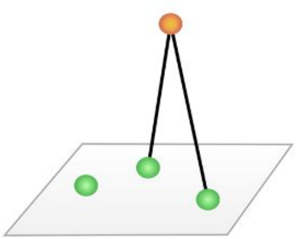

Part. Reco

- Compare DFEI (DF) to nominal HGNN (H1)
- ~5x higher perfect reconstruction

	Perfect reco.			Complete reco.			Not isolated			Part reco.		
Decay	DF	H1	H2	DF	H1	H2	DF	H1	H2	DF	H1	H2
inclusive beauty	4.7	22.4	21.9	6.1	20.1	20.6	76.1	44.1	44.1	13.1	13.4	13.4
$B^0 \to K^{*0}\mu\mu$	32.7	20.3	92.4	17.8	37.7	1.1	43.9	6.2	4.7	5.6	35.8	1.8
$B^0 \to K\pi$	38.1	47.4	91.6	0.0	0.0	0.0	54.7	10.2	7.0	7.2	42.4	1.4
$B^+ \to K\pi\pi$	35.6	23.7	94.5	10.3	26.3	0.2	46.5	8.5	4.7	7.6	41.5	0.6
$B^0_s \to J/\psi\phi$	31.3	22.8	91.8	20.3	44.3	1.7	44.3	9.9	5.0	4.1	22.9	1.5
$\Lambda_b \to \Lambda_c^+\pi$	22.2	27.5	68.3	8.6	9.4	24.4	37.4	7.3	5.2	31.8	55.7	2.1
$B^0 \to K\mu\mu$	36.2	21.0	93.5	10.4	28.1	0.3	45.9	8.4	4.9	7.5	42.5	1.2
$B^0_s \to D_s^-\pi$	33.0	57.7	67.5	7.1	11.6	23.0	53.5	13.1	7.0	6.4	17.6	2.6
$B^0 \to D^+D^-$	26.2	37.1	56.7	23.9	40.2	32.1	45.7	14.3	7.3	4.1	8.4	4.0
$\Lambda_b \to pK$	39.5	24.2	92.3	0.0	0.0	0.0	48.6	5.7	6.4	12.0	70.1	1.3
$\Lambda_b \to pK\mu\mu$	40.9	11.5	94.7	11.1	17.7	0.5	37.4	4.8	3.7	10.6	66.1	1.1

Reconstruction performance

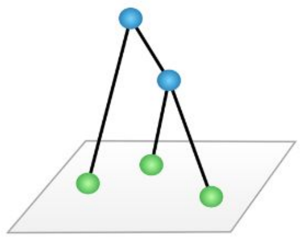

True decay

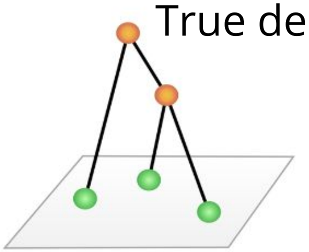

Perfect reco

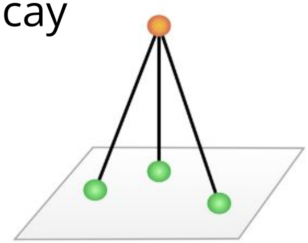

Complete reco

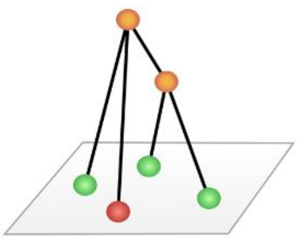

Not isolated

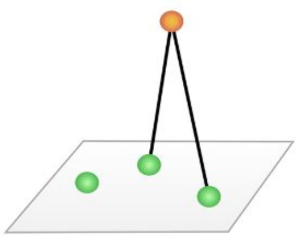

Part. Reco

- Compare DFEI (DF) to nominal HGNN (H1)
- ~5x higher perfect reconstruction

	Perfect reco.			Complete reco.			Not isolated			Part reco.		
Decay	DF	H1	H2	DF	H1	H2	DF	H1	H2	DF	H1	H2
inclusive beauty	4.7	22.4	21.9	6.1	20.1	20.6	76.1	44.1	44.1	13.1	13.4	13.4
$B^0 \to K^{*0}\mu\mu$	32.7	20.3	92.4	17.8	37.7	1.1	43.9	6.2	4.7	5.6	35.8	1.8
$B^0 \to K\pi$	38.1	47.4	91.6	0.0	0.0	0.0	54.7	10.2	7.0	7.2	42.4	1.4
$B^+ \to K\pi\pi$	35.6	23.7	94.5	10.3	26.3	0.2	46.5	8.5	4.7	7.6	41.5	0.6
$B_s^0 \to J/\psi\phi$	31.3	22.8	91.8	20.3	44.3	1.7	44.3	9.9	5.0	4.1	22.9	1.5
$\Lambda_b \to \Lambda_c^+\pi$	22.2	27.5	68.3	8.6	9.4	24.4	37.4	7.3	5.2	31.8	55.7	2.1
$B^0 \to K\mu\mu$	36.2	21.0	93.5	10.4	28.1	0.3	45.9	8.4	4.9	7.5	42.5	1.2
$B_s^0 \to D_s^-\pi$	33.0	57.7	67.5	7.1	11.6	23.0	53.5	13.1	7.0	6.4	17.6	2.6
$B^0 \to D^+D^-$	26.2	37.1	56.7	23.9	40.2	32.1	45.7	14.3	7.3	4.1	8.4	4.0
$\Lambda_b \to pK$	39.5	24.2	92.3	0.0	0.0	0.0	48.6	5.7	6.4	12.0	70.1	1.3
$\Lambda_b \to pK\mu\mu$	40.9	11.5	94.7	11.1	17.7	0.5	37.4	4.8	3.7	10.6	66.1	1.1

- HGNN H2 trained with extra 3k exclusive decays

Reconstruction performance

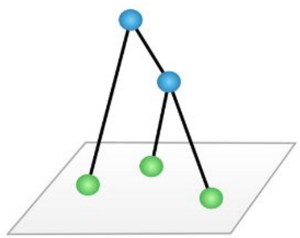

True decay

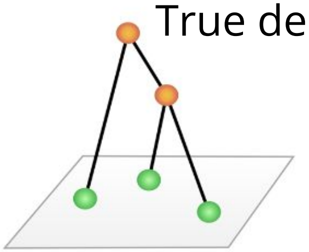

Perfect reco

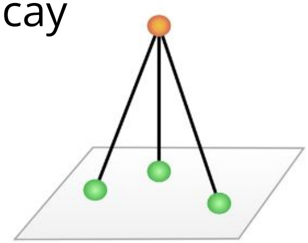

Complete reco

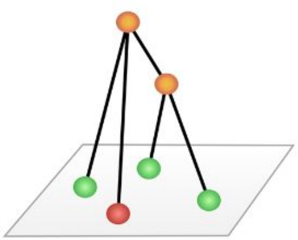

Not isolated

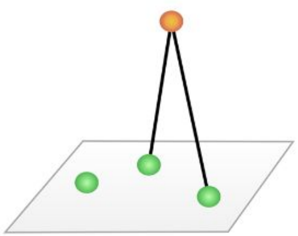

Part. Reco

- Compare DFEI (DF) to nominal HGNN (H1)
- ~5x higher perfect reconstruction

	Perfect reco.			Complete reco.			Not isolated			Part reco.		
Decay	DF	H1	H2	DF	H1	H2	DF	H1	H2	DF	H1	H2
inclusive beauty	4.7	22.4	21.9	6.1	20.1	20.6	76.1	44.1	44.1	13.1	13.4	13.4
$B^0 \to K^{*0}\mu\mu$	32.7	20.3	92.4	17.8	37.7	1.1	43.9	6.2	4.7	5.6	35.8	1.8
$B^0 \to K\pi$	38.1	47.4	91.6	0.0	0.0	0.0	54.7	10.2	7.0	7.2	42.4	1.4
$B^+ \to K\pi\pi$	35.6	23.7	94.5	10.3	26.3	0.2	46.5	8.5	4.7	7.6	41.5	0.6
$B_s^0 \to J/\psi\phi$	31.3	22.8	91.8	20.3	44.3	1.7	44.3	9.9	5.0	4.1	22.9	1.5
$\Lambda_b \to \Lambda_c^+\pi$	22.2	27.5	68.3	8.6	9.4	24.4	37.4	7.3	5.2	31.8	55.7	2.1
$B^0 \to K\mu\mu$	36.2	21.0	93.5	10.4	28.1	0.3	45.9	8.4	4.9	7.5	42.5	1.2
$B_s^0 \to D_s^-\pi$	33.0	57.7	67.5	7.1	11.6	23.0	53.5	13.1	7.0	6.4	17.6	2.6
$B^0 \to D^+D^-$	26.2	37.1	56.7	23.9	40.2	32.1	45.7	14.3	7.3	4.1	8.4	4.0
$\Lambda_b \to pK$	39.5	24.2	92.3	0.0	0.0	0.0	48.6	5.7	6.4	12.0	70.1	1.3
$\Lambda_b \to pK\mu\mu$	40.9	11.5	94.7	11.1	17.7	0.5	37.4	4.8	3.7	10.6	66.1	1.1

- HGNN H2 trained with extra 3k exclusive decays
- Generalises to other decays

PV association performance

Method			PV Association (%)		
method	task	edge type	track	beauty track	beauty hadron
min IP	-	-	95.56 ± 0.03	88.82 ± 0.21	96.14 ± 0.17
HGNN	$\mathcal{L}^{\mathrm{PV}}_{\mathrm{BCE}}$	tr-pv	97.83 ± 0.02	96.19 ± 0.14	97.60 ± 0.15
HGNN	$\mathcal{L}^{\mathrm{PV}}_{\mathrm{BCE}}$	tr-pv, tr-tr	99.83 ± 0.01	99.74 ± 0.04	99.85 ± 0.04
HGNN	$\mathcal{L}^{\mathrm{LCA}}_{\mathrm{CE}}, \mathcal{L}^{\mathrm{PV}}_{\mathrm{BCE}}, \mathcal{L}^{\mathrm{prune}}_{\mathrm{BCE}}$	tr-pv, tr-tr	99.88 ± 0.01	99.78 ± 0.04	99.85 ± 0.04

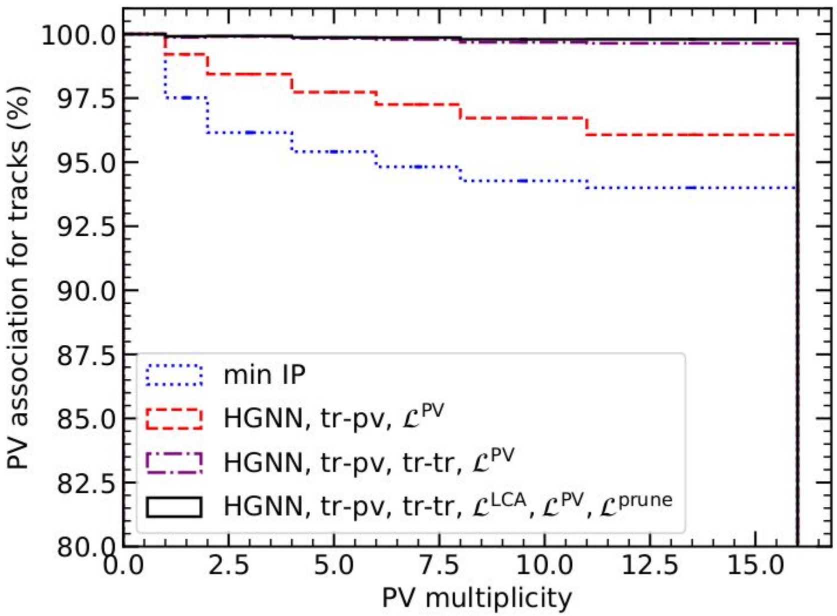

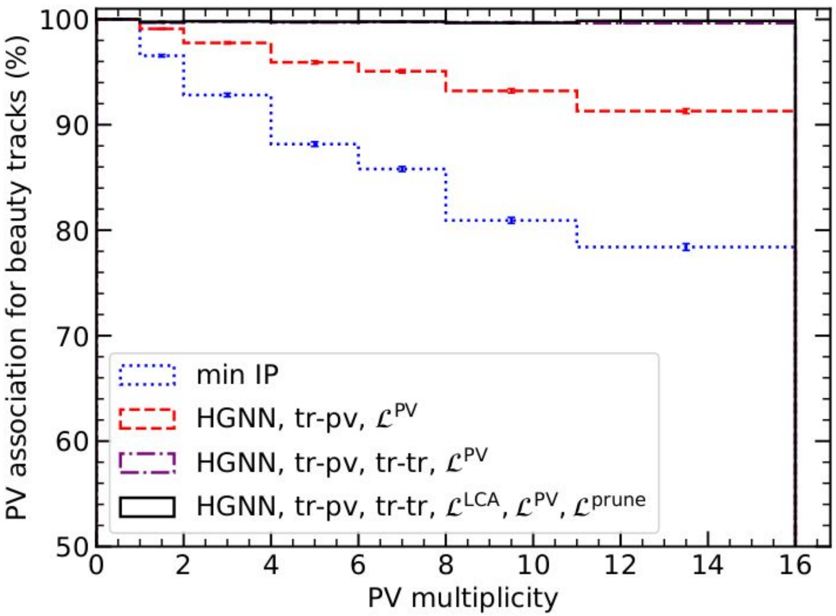

Timing and performance with pruning

- Early edge pruning:

$$\hat{y}^{e_{\mathrm{tr}}}_{1-3} > 10^{-4}$$

improves the scaling of inference time.

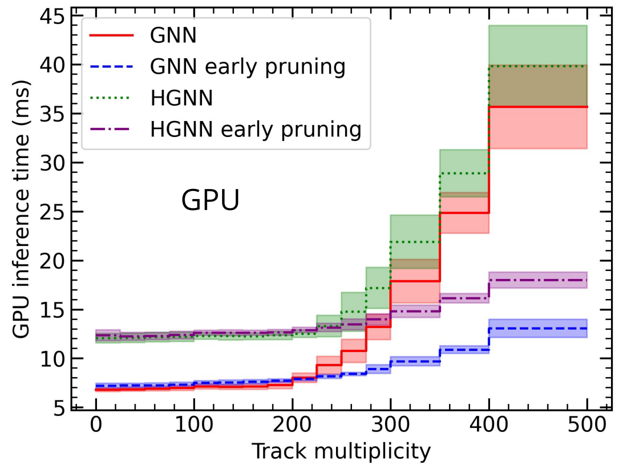

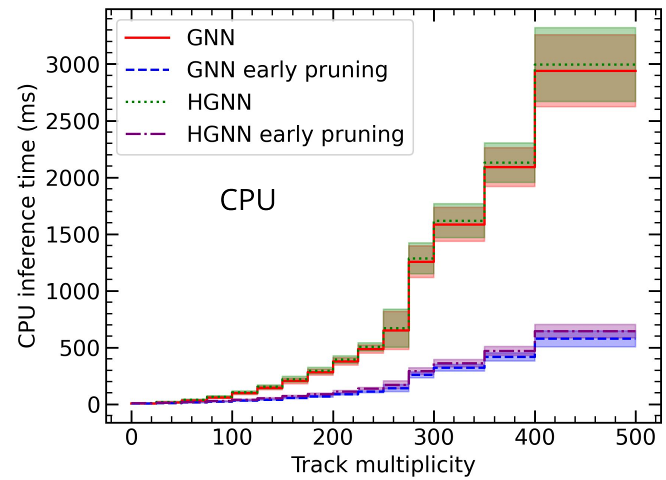

- Performance loss from early pruning can be mitigated with weighted message passing.

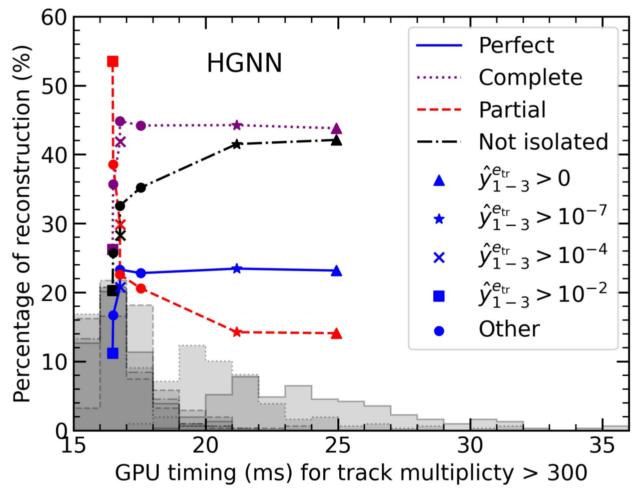

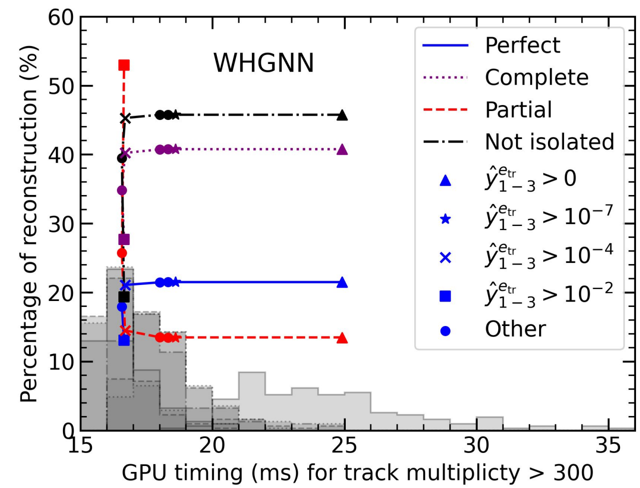

Conclusion

- The growing luminosity at the LHCb is challenging the reconstruction beauty hadron decays.

- Introduce a HGNN that jointly reconstructs beauty decays and assigns the correct primary vertex with high accuracy
  - Arxiv: arxiv2504.21844
  - Github: scalable_mtl_hgnn
  - Dataset: https://zenodo.org/records/15584745

- The percentage of perfect reconstruction on inclusive beauty decays ~5x higher than the previous DFEI algorithm.

- Early pruning allows for 2-3x (5x) speed up in GPU (CPU) inference time with minimal performance loss.

HGNN training and validation losses

$$\mathcal{L} = \underbrace{\mathcal{L}_{\mathrm{CE}}\left(e_{\mathrm{out}}, y^{\mathrm{LCA}}\right)}_{\text{LCA reco}} + \beta^{e_{\mathrm{tr}}} \sum_i^{n_{\mathrm{layers}}^{\mathrm{GNN}}} \underbrace{\mathcal{L}_{\mathrm{BCE}}\left(\hat{y}_i^{e_{\mathrm{tr}}}, y_i^{e_{\mathrm{tr}}}\right)}_{\text{Edge pruning}} + \beta^{v_{\mathrm{tr}}} \sum_i^{n_{\mathrm{layers}}^{\mathrm{GNN}}} \underbrace{\mathcal{L}_{\mathrm{BCE}}\left(\hat{y}_i^{v_{\mathrm{tr}}}, y_i^{v_{\mathrm{tr}}}\right)}_{\text{Node pruning}}$$

$$+ \beta^{e_{\mathrm{pv-tr}}} \sum_i^{n_{\mathrm{layers}}^{\mathrm{GNN}}} \underbrace{\mathcal{L}_{\mathrm{BCE}}\left(\hat{y}_i^{e_{\mathrm{pv-tr}}}, y_i^{e_{\mathrm{pv-tr}}}\right)}_{\text{PV association}}$$

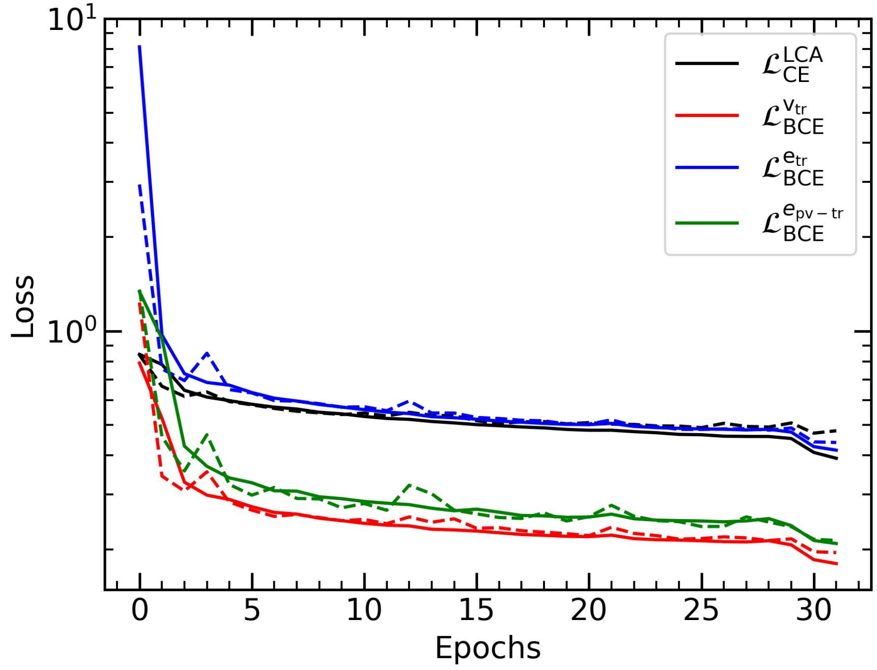

- Contributions of tasks to overall loss for the training.
- Training loss (solid)
- Validation loss (dashed)

Additional DFEI performance plots

- Selection efficiency for B particles and particles from the rest of the event.

- Confusion matrix shown below.

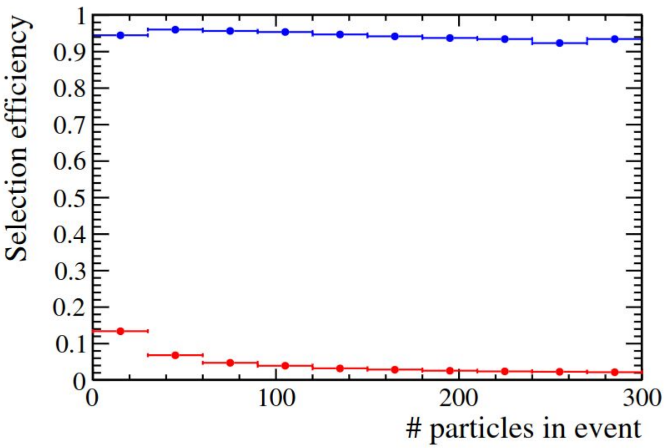

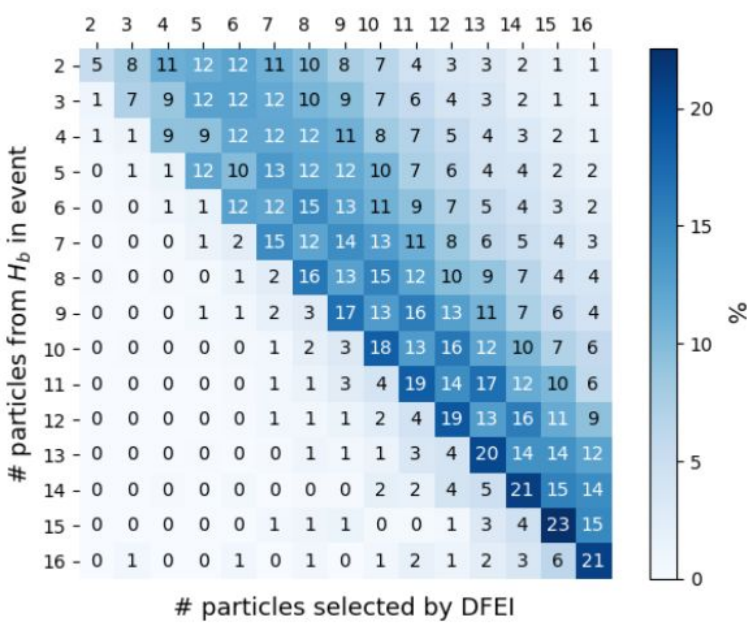

Confusion plot HGNN

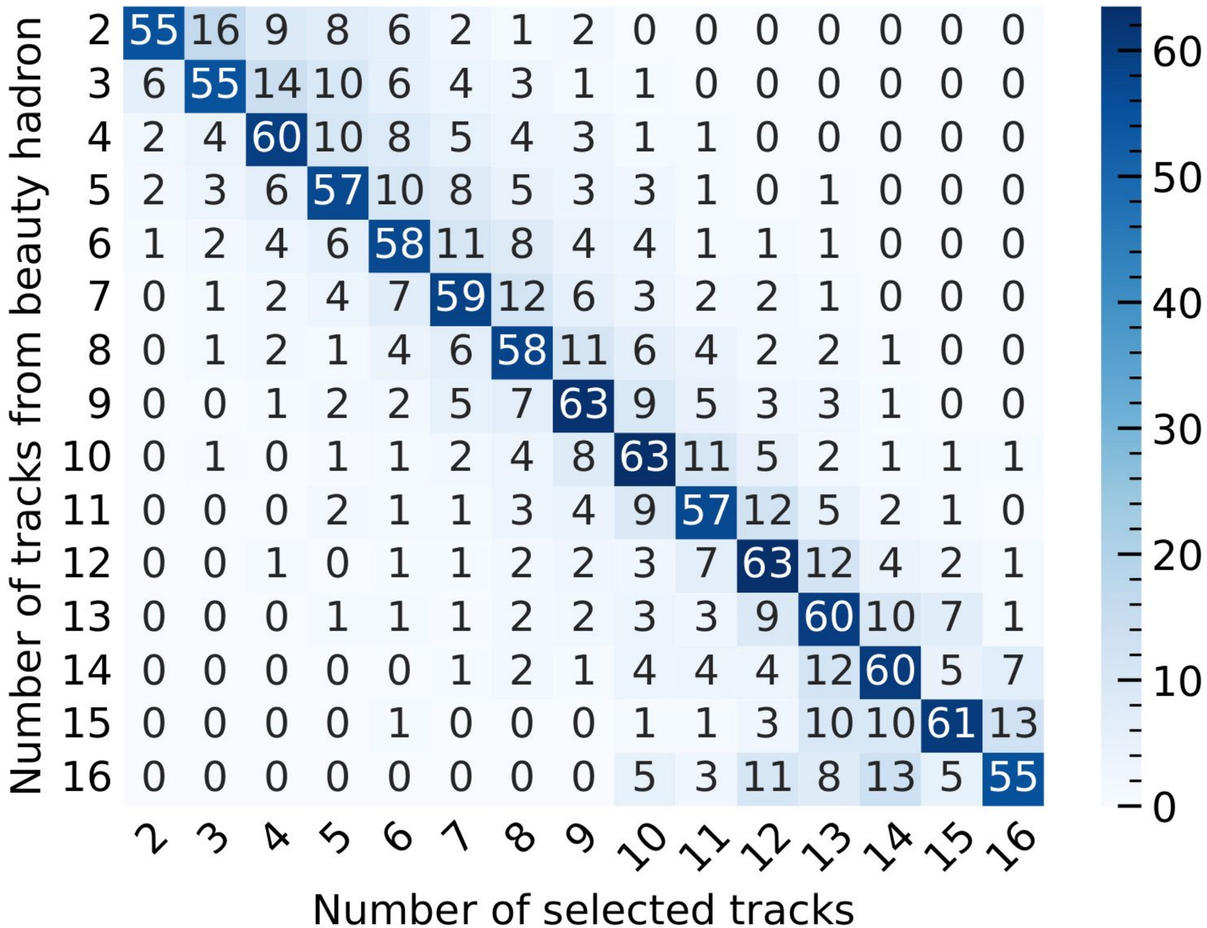

Classification accuracy with ablations

Model	Tasks	$\mathcal{L}_{\text{CE}}^{\text{LCA}}$	$y^{\text{LCA}} = 0$	$y^{LCA} = 1$	$y^{LCA} = 2$	$y^{LCA} = 3$
GNN	$\mathcal{L}_{\text{CE}}^{\text{LCA}}$	0.56	98.220 ± 0.001	68.0 ± 0.2	55.2 ± 0.1	79.9 ± 0.2
GNN	$\mathcal{L}_{\text{CE}}^{\text{LCA}}, \mathcal{L}_{\text{BCE}}^{\text{prune}}$	0.49	99.441 ± 0.001	75.5 ± 0.2	60.3 ± 0.1	83.2 ± 0.2
WGNN	$\mathcal{L}_{\text{CE}}^{\text{LCA}}$	0.60	97.955 ± 0.001	63.2 ± 0.2	53.5 ± 0.1	76.1 ± 0.3
WGNN	$\mathcal{L}_{\text{CE}}^{\text{LCA}}, \mathcal{L}_{\text{BCE}}^{\text{prune}}$	0.47	99.282 ± 0.001	76.9 ± 0.2	57.9 ± 0.1	85.6 ± 0.2
HGNN	$\mathcal{L}_{\text{CE}}^{\text{LCA}}$	0.54	98.826 ± 0.001	71.3 ± 0.2	51.6 ± 0.1	80.9 ± 0.2
HGNN	$\mathcal{L}_{\text{CE}}^{\text{LCA}}, \mathcal{L}_{\text{BCE}}^{\text{PV}}$	0.53	98.870 ± 0.001	71.8 ± 0.2	52.7 ± 0.1	82.5 ± 0.2
HGNN	$\mathcal{L}_{\text{CE}}^{\text{LCA}}, \mathcal{L}_{\text{BCE}}^{\text{PV}}, \mathcal{L}_{\text{BCE}}^{\text{prune}}$	0.49	99.289 ± 0.001	75.8 ± 0.2	61.4 ± 0.1	83.9 ± 0.2
WHGNN	$\mathcal{L}_{\text{CE}}^{\text{LCA}}$	0.58	98.683 ± 0.001	68.5 ± 0.2	52.8 ± 0.1	76.7 ± 0.2
WHGNN	$\mathcal{L}_{\text{CE}}^{\text{LCA}}, \mathcal{L}_{\text{BCE}}^{\text{PV}}$	0.51	98.959 ± 0.001	71.7 ± 0.2	54.8 ± 0.1	83.2 ± 0.2
WHGNN	$\mathcal{L}_{\text{CE}}^{\text{LCA}}, \mathcal{L}_{\text{BCE}}^{\text{PV}}, \mathcal{L}_{\text{BCE}}^{\text{prune}}$	0.46	99.274 ± 0.001	75.9 ± 0.2	61.3 ± 0.1	84.0 ± 0.2

Table 1. Comparison of the LCAG loss value and class accuracies in percent on the test dataset for various architectural ablations. The uncertainties on the LCAG class accuracies are statistical in nature.

Reconstruction performance

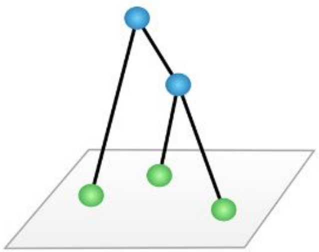

True decay

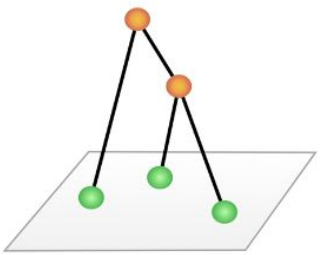

Perfect reco

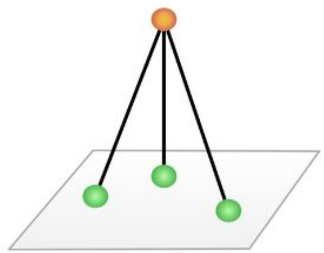

Complete reco

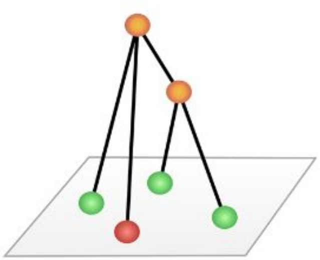

Not isolated

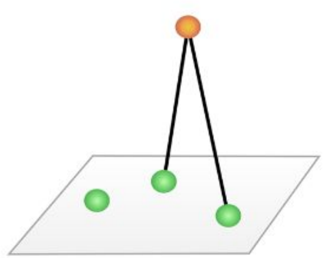

Part. Reco

Model	Perfect reco.	Complete reco.	Not isolated	Part. reco.
DFEI	4.7 ± 0.2	6.1 ± 0.2	76.1 ± 0.4	13.1 ± 0.3
GNN	21.6 ± 0.4	20.8 ± 0.4	43.8 ± 0.4	13.8 ± 0.3
WGNN	20.9 ± 0.4	20.0 ± 0.4	44.9 ± 0.4	14.2 ± 0.3
HGNN	22.4 ± 0.4	20.1 ± 0.4	44.1 ± 0.4	13.4 ± 0.3
WHGNN	21.5 ± 0.4	19.3 ± 0.3	45.8 ± 0.4	13.5 ± 0.3

	Perfect reco.			Complete reco.			Not isolated			Part reco.		
Decay	DF	H1	H2	DF	H1	H2	DF	H1	H2	DF	H1	H2
inclusive beauty	4.7	22.4	21.9	6.1	20.1	20.6	76.1	44.1	44.1	13.1	13.4	13.4
$B^0 \to K^{*0}\mu\mu$	32.7	20.3	92.4	17.8	37.7	1.1	43.9	6.2	4.7	5.6	35.8	1.8
$B^0 \to K\pi$	38.1	47.4	91.6	0.0	0.0	0.0	54.7	10.2	7.0	7.2	42.4	1.4
$B^+ \to K\pi\pi$	35.6	23.7	94.5	10.3	26.3	0.2	46.5	8.5	4.7	7.6	41.5	0.6
$B_s^0 \to J/\psi\phi$	31.3	22.8	91.8	20.3	44.3	1.7	44.3	9.9	5.0	4.1	22.9	1.5
$\Lambda_b \to \Lambda_c^+\pi$	22.2	27.5	68.3	8.6	9.4	24.4	37.4	7.3	5.2	31.8	55.7	2.1
$B^0 \to K\mu\mu$	36.2	21.0	93.5	10.4	28.1	0.3	45.9	8.4	4.9	7.5	42.5	1.2
$B_s^0 \to D_s^-\pi$	33.0	57.7	67.5	7.1	11.6	23.0	53.5	13.1	7.0	6.4	17.6	2.6
$B^0 \to D^+D^-$	26.2	37.1	56.7	23.9	40.2	32.1	45.7	14.3	7.3	4.1	8.4	4.0
$\Lambda_b \to pK$	39.5	24.2	92.3	0.0	0.0	0.0	48.6	5.7	6.4	12.0	70.1	1.3
$\Lambda_b \to pK\mu\mu$	40.9	11.5	94.7	11.1	17.7	0.5	37.4	4.8	3.7	10.6	66.1	1.1

DF - DFEI
H1 - nominal HGNN training
H2 - training with 3k exclusive decays added from upper half of table